J Biochem Tech (2019) (4): 16-25
ISSN: 0974-2328

Biosynthesis of silver nanoparticles using Arachis Pintoi extract and its antibacterial activity

Nguyen Phung Anh, Phan Ngo Minh Quang, Duong Trong Van, Luong Thi Cam Van, Duong Nhat Linh, Nguyen Van Minh, Vuong Phu Tai, Nguyen Tri*

Received: 22 May 2019 / Received in revised form: 17 October 2019, Accepted: 25 October 2019, Published online: 27 December 2019

Abstract

An operational and eco-friendly technique was applied for the synthesis of silver nanoparticles (AgNPs) utilizing *Arachis pintoi (A. pintoi)* extract as a reducing agent. The features of synthesized AgNPs were investigated utilizing XRD, SEM, TEM, and FT-IR. The formation of AgNPs was verified by UV-Vis spectroscopy at the wavelength range of 400–450 nm. The proper conditions for AgNPs synthesis were determined such as the $AgNO_3$ concentration of 1.75 mM, the volume ratio of $AgNO_3$ solution/*A. pintoi* extract of 4.0/1.0, stirring rate of 300 rpm, and the synthesis duration of 90 minutes. X-ray diffraction demonstrated a face-centered cubic structure of AgNPs with highly crystalline nature. FT-IR confirmed that flavonoids, phenolic acids, and alkaloid molecules can be bound to AgNP acted both as the reducing and stabilizing agents. SEM and TEM images revealed that obtained AgNP was nearly spherical in shape and uniform in size distribution with the average size of 11.4 nm. AgNPs showed effective antibacterial activity against *Staphylococcus aureus* with the average inhibition zone diameters of 14 mm and the MIC value of 18.9 µg/mL. Furthermore, its antibacterial activity on the mouse pad was tested against *S. aureus*.

Key words: Biosynthesis, silver nanoparticles, *Arachis pintoi*, antibacterial, *Staphylococcus aureus*

Nguyen Phung Anh
Institute of Chemical Technology, 01 Mac Dinh Chi Str., HCM City, Vietnam.

Phan Ngo Minh Quang, Duong Trong Van
Nguyen Thuong Hien High School, 544 CMT8 Str., HCM City, Vietnam

Luong Thi Cam Van, Duong Nhat Linh, Nguyen Van Minh, Vuong Phu Tai
Ho Chi Minh City Open University, 97 Vo Van Tan Str., HCM City, Vietnam

Nguyen Tri*
Institute of Chemical Technology, 01 Mac Dinh Chi Str., HCM City, Vietnam
Ho Chi Minh City Open University, 97 Vo Van Tan Str., HCM City, Vietnam.

***Email**: ntri @ ict.vast.vn

Introduction

Infections are one of the serious issues that are influencing human health. Infections are published both in hospital-acquired and community-acquired settings (Millar, 2019). Treatment for the issues remains challenging because of the emergence of multi-drug resistant strains (Ferguson, 2018). *Staphylococcus aureus (S. aureus)* is a major bacterial human pathogen that leads to a wide range of clinical manifestations (Roberts and Buikstra, 2019). It was reported that the bacterium is present in the environment and normal flora of humans, such as mucous membranes and skin of the most healthy human (Boldock and Surewaard, 2018). It is predicted that up to half of all adults are colonized, and almost 15 percent of the population persistently carry *S. aureus* (Taylor and Unakal, 2017). On healthy skin, *S. aureus* does not usually result in infection. Nevertheless, if it is permitted to enter the bloodstream or internal tissues, these bacteria may cause a variety of potentially serious infections (Lowy, 1998).

Infection at the office is one of the issues of concern. A mouse pad is a type of computer accessory and is used on a regular basis for working people. The high-polymer materials used for making the mouse pad are not dirt-resistant and are hard to clean. Hands and wrists of people often touch the mouse pad when they utilize a mouse, and their hands touch the other parts of their body most often. Consequently, mouse pads that are simply contaminated by bacteria may be unsafe for people's health. So, the introduction of antibacterial agents incorporated into the surface of this mouse pad inhibited the growth of bacteria. To keep the area cleaner is one of the research areas that receive present attention.

The development of *S. aureus* bacterial resistance to currently existing antibiotics is one of the most serious problems. Therefore, it is crucial to find new antibacterial agents with low cost and adverse effects.

Nanotechnology is one of the ways for the development of efficient antibacterial agents (Sing et al., 2008; Esteban-Tejeda et al., 2009). Silver nanoparticles (AgNPs) are a very noteworthy part of nanotechnology as they do not induce modification on living cells and are not able to cause microbial resistance (Shrivastava et al., 2007; Vasilev et al.., 2010). Although there are various conventional approaches utilized to obtain AgNPs (Tan et al., 2002; Starowicz et al., 2006; Esumi et al., 1990; Henglein, 2001; Zhu et al., 2000; Pastoriza-Santos and Liz-

Marzán, 2002), green chemistry and biosynthetic techniques have become more attractive ways. These unconventional techniques utilize either biological microorganisms (Vahabi et al., 2011; Sharma et al., 2010), i.e. yeasts, marine algae, bacteria, fungi, or different aqueous plant extracts (Mahitha et al., 2011; Babu and Prabu, 2011). Biosynthesis has various advantages as they are inexpensive, eco-friendly, and not require high pressure, energy, temperature or the utilization of toxic chemical reagents. Nevertheless, plant-mediated synthesis of AgNPs is more advantageous compared to methods utilizing microorganisms because they can be easily improved, are less biohazardous and not involving the elaborate stage of growing cell cultures (Raut Rajesh et al., 2009). Plant parts like seeds (Bar et al., 2009), leaf (Narayanan and Sakthivel, 2008), bark (Sathishkumar et al., 2009), stem (Daisy and Saipriya, 2012), and fruit extracts (Ankamwar et al., 2005) have been effectively used for synthesizing AgNPs.

Arachis pintoi (*A. pintoi*) is a tropical legume, originated from South America and has been widespread in the subtropics and wet tropics. It has been introduced to many areas including Argentina, Australia, Colombia and the USA, and countries in South-East Asia, Central America, and the Pacific. *A. pintoi* can be utilized as a ground cover as well as an ornament. It is compatible with aggressive grasses such as *Brachiaria* and is tolerant of heavy grazing. Previous chemical analyses of the plant indicated the presence of phytosterols, flavonoids, phenolic acids, triterpenes, alkaloids, fatty acids, etc. (Lopes et al., 2011). However, much less investigation of AgNPs synthesis has been reported to date utilizing *A. pintoi* extract as a combined reducing and stabilizing agent.

In this paper, AgNPs were synthesized by the reduction of AgNO3 solution utilizing *A. pintoi* extract as a combined reducing and stabilizing agent. Effects of the synthesis duration, the volume ratio of $AgNO_3$ solution/*A. pintoi* extract, stirring rate and $AgNO_3$ concentration of AgNPs were assessed. The obtained AgNPs' properties were investigated, and the antibacterial activity was evaluated against *S. aureus*. Its antibacterial activity on mouse pad against *S. aureus* was also examined.

Material and Methods

Synthesis of AgNPs

Fig. 1 illustrates the green synthesis and characterization of AgNPs from *A. pintoi* extract. *A. pintoi* plants (both leaves and stems) were collected and washed several times with distilled water to eliminate the dust particles, and then ground to the fine powder in distilled water with the mass ratio of *A. pintoi*/water being 1/10. The mixture was boiled at 70 ºC for 2 hours to extract reducing agents in the presence of leaves and stems of *A. pintoi*. The obtained extract was cooled to room temperature and then filtered with Whatman filter paper 0.22 μm before centrifuging at 5,000 rpm for 30 min to eliminate the heavy biomaterials. The extract was stored in the refrigerator at 4 ºC for further experiments.

The AgNPs synthesis was performed by mixing silver nitrate ($AgNO_3$, Merck, >99.8%) solution with *A. pintoi* extract under stirring at room temperature and illuminated by the sunlight. The effects of the factors such as the $AgNO_3$ concentration, the volume ratio of $AgNO_3$ solution/*A. pintoi* extract, the stirring rate, and the duration of AgNPs synthesis were surveyed.

The mousepad was cut into small pieces with a size of 4 cm^2 (2 cm × 2 cm). Then, the as-prepared AgNPs were implanted on the pieces of mouse pad according to the following procedure. Firstly, the synthesized AgNPs solution was mixed with 0.5 wt.% of cloth starching and heated at 80 °C for 1 hour. Nextly, the mouse pads were soaked in this solution with 30 minutes of ultrasound. Then, it was taken out and dried at 60 °C under vacuum pressure (–700 mmHg) within 12 hours to obtain the pieces of mouse pad coated with AgNPs. The concentrations of AgNPs coated on mouse pad were tested at 0.5 and 1.0 wt.% denoted as 0.5 wt.% Ag/MP and 1.0 wt.% Ag/MP.

Characterization of AgNPs

The presence of synthesized AgNPs in the solution was determined by UV-Vis spectrophotometer (UV-1800, Shimadzu) in the range of 200–800 nm. The crystalline structure of the synthesized AgNPs powder dried at 60 °C under vacuum pressure (–700 mmHg) within 12 hours was confirmed by X-ray diffractometer (Bruker D2 Pharser X-Ray Diffractometer) with Cu Kα radiation (40 kV, 40 mA) and the scanning step of 0.02°. The FT-IR spectra were measured using Bruker Tensor 2700 FTIR spectrometer operated in the range of 400–4,000 cm^{-1} with a resolution of 4 cm^{-1} using thin transparent KBr pellets to describe the functional groups of synthesized AgNPs. The elemental analysis of the synthesized nanoparticles was carried out utilizing EDX (JED-2300, Akishima). The size and morphology of AgNPs were assessed using TEM (JEOL 1400). According to the TEM image, by utilizing the ImageJ software, the size distribution of AgNPs was determined.

Antibacterial activity of samples

The synthesized AgNPs were tested for antibacterial activity against *S. aureus* ATCC 43300 (MRSA) utilizing an agar well diffusion technique. Pre-cultivation of the bacteria was performed on nutrient agar slant at 37 °C in 24 hours by pricking a single colony of microbial strains. The bacterial cultures were then diluted from slants in 0.85% NaCl with a density equivalent to 0.5 McFarland standard (1.5×10^8 $CFU.mL^{-1}$) to prepare the inoculum of each strain. Later, Muller Hinton Agar plates were prepared and four wells of 6 mm in diameter were provided on each agar plate. 70 μL of synthesized AgNPs solution was poured into three out of the four wells on each plate. The remaining well was utilized as a control. After 15 minutes for AgNPs to diffuse into the agar, the samples were maintained at 37 °C for 24 hours. Finally, the diameter of the inhibition zone around the agar was determined.

To determine the minimum inhibitory concentration (MIC) of

AgNPs against *S. aureus*, various concentrations of AgNPs (N/2, N/4, N/8, N/16, N/32, N/64, and N/128 with N as the initial concentration of AgNPs solution in deionized water; N = 151.2 µg/mL) were prepared by diluting AgNPs solution with deionized water. Subsequently, the diluted samples were mixed with the sterile nutrient agar. By using sterile sticks, five points on agar plates mixed with AgNPs samples from low to high concentrations were inoculated with the standardized inoculum of bacteria with 1.5×10^7 CFU/ml. A plate of the sterile nutrient agar without AgNPs was utilized as control (Wayne, 2013). Finally, the plates were kept at 37 °C for 24 hours. The lowest concentration of AgNPs inhibiting the growth of tested bacteria was considered as the MIC value (Washington and Wood, 1995).

A piece of mouse pad coated with AgNPs was put in Petri plates in a UV stove (λ = 254 nm) within 2 hours to kill all bacteria. 50 µL of the prepared bacterial solution was filled in a plate where the nutrient agar slant was previously prepared in the area of the sample. The sample was put into the prepared agar plate at the position where the sample surface was in contact with the surface of a nutrient agar plate. The plate was preserved at 37 °C in 24 hours. The sample uncoated with AgNPs was used as a control. The antibacterial activity of samples was evaluated by the levels of bacterial colonies not detected on the surface of samples.

Results and Discussion

Synthesis of AgNPs

The impact of time on the formation of AgNPs was shown in Fig. 2a. The production of AgNPs was taken placed with the presence of direct sunlight after 30 minutes; the band indicating the presence of AgNPs in the solution was observed in the range of 400–450 nm. When the synthesis time increased, the absorbance peak was broadened, revealing a high conversion of silver ions to metallic silver nanoparticles. Prolonging the reaction time up to 90 min resulted in an outstanding enhancement in the plasmon intensity indicating that large amounts of silver ions were reduced and utilized for AgNPs formation. In the synthesis duration up to 120 and 150 min, the formed silver nanoparticles decreased slightly which could be attributed to some aggregation of the formed silver nanoparticles. Therefore, 90 minutes was selected as the optimal reduction time for the AgNPs synthesis process utilizing *A. pintoi* extract as a combined reducing and stabilizing agent.

With the volume ratio of $AgNO_3$ solution/*A. pintoi* extract at 4.0/1.0, the production of AgNPs reached the highest performance (Fig. 2b). The components in the extract had effectively reduced the Ag^+ ions to Ag^o with high extract concentrations, and provided enough capping agent for the stabilization of the synthesized nanoparticles through steric hindrance so, inhibiting their aggregation (Rastogi and Arunachalam, 2013). These findings were a good agreement with those obtained by Subramanian *et al*.

In Fig. 2c, the $AgNO_3$ concentration increased as using the initial Ag^+ concentrations from 1.25 to 1.75 mM. However, the production of AgNPs decreased in the case of a continuous increase in $AgNO_3$ concentration up to 2 mM. At a low concentration, nanoparticles have appeared no more, while nanoparticles have been formed at a higher concentration (Moosa et al., 2015). However, when silver concentrations were too high, silver nanoparticles agglomerated together reducing the efficiency of the process.

Fig. 2d demonstrates that the production of the AgNPs increased when the stirring rate increased from 100 to 300 rpm. However, when the stirring rate continuously rose up to 400 rpm, this formation remained almost unchanged. Because of the increase in nanostructure concentration, stronger mixing was essential to provide uniform heat and mass transfer (Hemmati and Barkey, 2017). So, the stirring rate of 300 rpm was consistent for the synthesis process.

So, the suitable conditions for AgNPs synthesis using *A. pintoi* extract as a reducing and stabilizing agent were determined such as $AgNO_3$ concentration of 1.75 mM, the volume ratio of $AgNO_3$ solution/*A. pintoi* extract of 4.0/1.0, stirring rate of 300 rpm, and the synthesis duration of 90 minutes.

Characterization of AgNPs

AgNPs solution was synthesized using *A. pintoi* extract, and AgNPs powder is depicted in Fig. 3. The spectrum for *A. pintoi* extract showed typical broad O-H stretching (3600–3300 cm^{-1}) and C=O stretching (1730–1690 cm^{-1}), suggesting the presence of flavonoids, phenolic acids, and alkaloids in the extract that acted both as the reducing and stabilizing agents. The difference was not much on samples of pure extract and AgNPs solution. This could be due to the fact that the compounds of extract covered the peaks of the silver nanoparticles by the functional groups present in the extract, so the production of the peaks of the silver nanoparticles was unclear. Nevertheless, compared to the extract, the FT-IR spectrum of AgNPs solution indicated the existence of weaker signals, verifying the components of the extract reacted to form silver nanoparticles, so the concentration of the extract was significantly decreased. On the FT-IR spectrum of AgNPs powder, a band centered at 2950 cm^{-1} was related to the axial stretching of C–H bonds, a band centered at 1810 cm^{-1} was attributed to the axial stretching of C=O bonds of the acetamide groups, a band at 1420 cm^{-1} corresponded to the symmetric angular deformation of CH_3, the absorption at 1340–1340 cm^{-1} has been assigned to C–H bending and CH_2 wagging, and the bands around 1200–1300 cm^{-1} are related to N–H bend amines. There was broadband in the wavenumber range of 1150–890 cm^{-1} demonstrating the polysaccharide skeleton, including the vibrations of the C–O and C–O–C stretching, and glycoside bonds. From the analysis of FT-IR examinations, it was confirmed that the flavonoids and alkaloids components together with phenolic acids in *A. pintoi* extract possibly did dual functions for the production and stabilization of AgNPs.

X-ray diffraction analysis (XRD) result of AgNPs synthesized from *A. pintoi* extract was shown in Fig. 4. Several Bragg reflections with 2θ = 38.5, 46.7, 64.5, and 77.3° associated with the sets of (111), (200), (220) and (311) reflection planes are obtained, which may be recorded as the band for the face-centered cubic (JCPDS card No. 89-3722) structure of AgNPs. Therefore, XRD verifies that the samples are pure AgNPs with a highly crystalline nature. Besides, a few intense and unassigned peaks at 2θ = 28.1, 32.4, 55.6, and 57.0° in the vicinage of silver peaks exhibited the presence of bio-organic phase crystals (AbdelHamid et al., 2013), which were present in the extract and responsible for silver ions reduction and stabilization of nanoparticles. The average crystal size of the sample at the (111) crystallographic plane can be determined by the Debye–Scherrer equation (Patterson, 1939) with K = 0.94. The mean particle size calculated from the XRD patterns is 11.4 nm.

SEM images obtained from the sample showed the presence of nano-sized particles (Fig. 5a). This result showed that the particles were spherical in shape and the size of the prepared nanoparticles reached a range of 5–50 nm. The size was more than the average crystal size determined by Debye–Scherrer equation on X-ray diffraction as a result of the bio-organics in the extract which were bound in the surface of the nanoparticles or AgNPs particles linked together. TEM image revealed further insight into the morphology and size details of the silver nanoparticles. The result of the TEM image of the AgNPs sample (Fig. 5b) also demonstrated that nanoparticles were highly dispersed with a spherical shape. The image clearly revealed a bio-organic layer coating around AgNPs. This layer was because of the surrounded phytochemicals in the extracts that served as a capping agent to prevent agglomeration. From the TEM image, by utilizing the ImageJ software, the size distribution of the AgNPs sample was elucidated in Fig. 5c, and the average size of the obtained AgNPs was assessed at approximately 11.4 nm. This finding was consistent with the XRD result.

Antibacterial activity of samples

The antibacterial activity of the AgNP sample was evaluated against *S. aureus* bacterial strain on an agar plate. Fig. 6 depicts the inhibition zone of the synthesized AgNP sample against the bacteria. The average inhibition zone diameters against *S. aureus* was 14 mm. It has been stated that AgNPs can quickly attach to the bacterial cell membrane and penetrate the cytoplasm (López-Esparza et al., 2016). This produced structural modifications in the cell, and consequently the elimination of this organism. The average inhibition zone diameter of AgNPs against *S. aureus* bacteria in this work was higher than that of previous publication utilizing *Melissa officinalis* leaf extract (6–11.5 mm) (De Jesús Ruíz-Baltazar et al., 2017). The smaller size of AgNPs exhibited higher antibacterial features due to higher surface area and faster release of silver ions.

The antibacterial activities of the AgNPs sample were further determined by the MIC value. Fig. 7 depicts the inhibition zone against *S. aureus* treated with AgNPs solutions under various concentrations. It was observed that the exponential phase of bacteria delayed in the existence of AgNPs and this phenomenon was more obvious with the enhancement of AgNPs concentration. The sample could delay the exponential phase of *S. aureus* and could completely inhibit the bacterial growth at a MIC of 18.9 µg/mL (N/8).

As seen in Fig. 8, both mouse pads coated with AgNPs had high antimicrobial activity against *S. aureus*. No colonies appeared on the surface of both samples coated with 0.5 wt.% and 1.0 wt.% AgNPs synthesized by utilizing *A. pintoi* extract. Besides, the antibacterial activity of samples can also be found in the antibacterial width of 3.0–3.5 mm on four edges of the pieces of mouse pad coated with AgNPs. Compared with mouse pad coated with 0.5 wt.% AgNPs (0.5 wt.%Ag/MP), the antibacterial activity of the one coated with 1.0 wt.% AgNPs was not much stronger. With these promising findings, the process is potential to be expanded in the green synthesis where the AgNPs could be utilized for various antibacterial applications including household appliances, personal belongings, self-sterilizing textiles, etc.

Conclusion

The reduction of silver ions into silver nanoparticles by green chemistry utilizing *A. pintoi* extract under direct sunlight at room temperature was verified to be efficient and rapid. The XRD, SEM, and TEM images of silver nanoparticles confirmed the production of highly crystalline particles possessing a spherical shape with the size in a range of 4-24 nm. The silver nanoparticles synthesized utilizing *A. pintoi* extracts as a combined reducing and stabilizing agent revealed efficient antibacterial activity against *S. aureus* with the average inhibition zone diameters of 14 mm and the MIC value of 16.52 µg/mL. Hence, the properties of silver nanoparticles obtained from *A. pintoi* extract can unfasten new pathways in the development of new antibacterial agents derived from plant drugs. The mouse pad coated with silver nanoparticles synthesized from *A. pintoi* extract as an eco-friendly product has the potential to provide the health of office workers.

References

AbdelHamid, A. A., Al-Ghobashy, M. A., Fawzy, M., Mohamed, M. B., & Abdel-Mottaleb, M. M. (2013). Phytosynthesis of Au, Ag, and Au–Ag bimetallic nanoparticles using aqueous extract of sago pondweed (Potamogeton pectinatus L.). *ACS Sustainable Chemistry & Engineering*, *1*(12), 1520-1529.

Ankamwar, B., Damle, C., Ahmad, A., & Sastry, M. (2005). Biosynthesis of gold and silver nanoparticles using Emblica officinalis fruit extract, their phase transfer and transmetallation in an organic solution. *Journal of nanoscience and nanotechnology*, *5*(10), 1665-1671.

Babu, S. A., & Prabu, H. G. (2011). Synthesis of AgNPs using the extract of Calotropis procera flower at room temperature. *Materials Letters*, *65*(11), 1675-1677.

Bar, H., Bhui, D. K., Sahoo, G. P., Sarkar, P., Pyne, S., & Misra, A. (2009). Green synthesis of silver nanoparticles using seed extract of Jatropha curcas. *Colloids and Surfaces A: Physicochemical and Engineering Aspects*, *348*(1-3), 212-216.

Boldock, E., Surewaard, B. G., Shamarina, D., Na, M., Fei, Y., Ali, A., ... & Prajsnar, T. K. (2018). Human skin commensals augment Staphylococcus aureus pathogenesis. *Nature microbiology*, 1.

Daisy, P., & Saipriya, K. (2012). Biochemical analysis of Cassia fistula aqueous extract and phytochemically synthesized gold nanoparticles as hypoglycemic treatment for diabetes mellitus. *International journal of nanomedicine*, *7*, 1189.

de Jesús Ruíz-Baltazar, Á., Reyes-López, S. Y., Larrañaga, D., Estévez, M., & Pérez, R. (2017). Green synthesis of silver nanoparticles using a Melissa officinalis leaf extract with antibacterial properties. *Results in physics*, *7*, 2639-2643.

Esteban-Tejeda, L., Malpartida, F., Esteban-Cubillo, A., Pecharromán, C., & Moya, J. S. (2009). Antibacterial and antifungal activity of a soda-lime glass containing copper nanoparticles. *Nanotechnology*, *20*(50), 505701.

Esumi, K., Tano, T., Torigoe, K., & Meguro, K. (1990). Preparation and characterization of bimetallic palladium-copper colloids by thermal decomposition of their acetate compounds in organic solvents. *Chemistry of Materials*, *2*(5), 564-567.

Ferguson, N. M. (2018). Challenges and opportunities in controlling mosquito-borne infections. *Nature 559*: 490-497.

Hemmati, S., & Barkey, D. P. (2017). Parametric study, sensitivity analysis, and optimization of polyol synthesis of silver nanowires. *ECS Journal of Solid State Science and Technology*, *6*(4), P132-P137.

Henglein, A. (2001). Reduction of Ag (CN) 2-on silver and platinum colloidal nanoparticles. *Langmuir*, *17*(8), 2329-2333.

Lopes, R. M., Agostini-Costa, T. D. S., Gimenes, M. A., & Silveira, D. (2011). Chemical composition and biological activities of Arachis species. *Journal of agricultural and food chemistry*, *59*(9), 4321-4330.

López-Esparza, J., Espinosa-Cristóbal, L. F., Donohue-Cornejo, A., & Reyes-López, S. Y. (2016). Antimicrobial activity of silver nanoparticles in polycaprolactone nanofibers against gram-positive and gram-negative bacteria. *Industrial & Engineering Chemistry Research*, *55*(49), 12532-12538.

Lowy, F. D. (1998). Staphylococcus aureus infections. *New England journal of medicine*, *339*(8), 520-532.

Mahitha, B., Raju, B. D. P., Dillip, G. R., Reddy, C. M., Mallikarjuna, K., Manoj, L., ... & Sushma, N. J. (2011). Biosynthesis, characterization and antimicrobial studies of AgNPs extract from Bacopa monniera whole plant. *Digest Journal of Nanomaterials and Biostructures*, *6*(2), 587-594.

Millar, M. (2019). *Device-associated infections*. (Ed) Tutorial Topics in Infection for the Combined Infection Training Programme, Edn.

Moosa, A. A., Ridha, A. M., & Al-Kaser, M. (2015). Process parameters for green synthesis of silver nanoparticles using leaves extract of Aloe vera plant. *Int J Multi Curr Res*, *3*, 966-75.

Narayanan, K. B., & Sakthivel, N. (2008). Coriander leaf mediated biosynthesis of gold nanoparticles. *Materials Letters*, *62*(30), 4588-4590.

Pastoriza-Santos, I., & Liz-Marzán, L. M. (2002). Formation of PVP-protected metal nanoparticles in DMF. *Langmuir*, *18*(7), 2888-2894.

Patterson, A. L. (1939). The Scherrer formula for X-ray particle size determination. *Physical review*, *56*(10), 978.

Rastogi, L., & Arunachalam, J. (2013). Green synthesis route for the size controlled synthesis of biocompatible gold nanoparticles using aqueous extract of garlic (Allium sativum). *Advanced Materials Letters*, *4*(7), 548-555.

Raut Rajesh, W., Lakkakula Jaya, R., Kolekar Niranjan, S., Mendhulkar Vijay, D., & Kashid Sahebrao, B. (2009). Phytosynthesis of silver nanoparticle using Gliricidia sepium (Jacq.). *Current Nanoscience*, *5*(1), 117-122.

Roberts, C. A. & Buikstra, J. E. (2019). Bacterial infections: Elsevier.

Sathishkumar, M., Sneha, K., Won, S. W., Cho, C. W., Kim, S., & Yun, Y. S. (2009). Cinnamon zeylanicum bark extract and powder mediated green synthesis of nano-crystalline silver particles and its bactericidal activity. *Colloids and Surfaces B: Biointerfaces*, *73*(2), 332-338.

Sharma, S., Ahmad, N., Prakash, A., Singh, V. N., Ghosh, A. K., & Mehta, B. R. (2010). Synthesis of crystalline Ag nanoparticles (AgNPs) from microorganisms. *Materials Sciences and Applications*, *1*(01), 1.

Shrivastava, S., Bera, T., Roy, A., Singh, G., Ramachandrarao, P., & Dash, D. (2007). Characterization of enhanced antibacterial effects of novel silver nanoparticles. *Nanotechnology*, *18*(22), 225103.

Singh, M., Singh, S., Prasad, S., & Gambhir, I. S. (2008). Nanotechnology in medicine and antibacterial effect of silver nanoparticles. *Digest Journal of Nanomaterials and Biostructures*, *3*(3), 115-122.

Starowicz, M., Stypuła, B., & Banaś, J. (2006). Electrochemical synthesis of silver nanoparticles. *Electrochemistry Communications*, *8*(2), 227-230.

Subramanian, R., Subbramaniyan, P., & Raj, V. (2013). Antioxidant activity of the stem bark of Shorea roxburghii and its silver reducing power. *SpringerPlus*, *2*(1), 28.

Tan, Y., Wang, Y., Jiang, L., & Zhu, D. (2002). Thiosalicylic acid-functionalized silver nanoparticles synthesized in one-phase system. *Journal of colloid and interface science*, *249*(2), 336-345.

Taylor, T. A., & Unakal, C. G. (2018). Staphylococcus Aureus.[Updated 2017 Oct 9]. *StatPearls [Internet]. Treasure Island (FL): StatPearls Publishing*.

Vahabi, K., Mansoori, G. A., & Karimi, S. (2011). Biosynthesis of silver nanoparticles by fungus Trichoderma reesei (a route for large-scale production of AgNPs). *Insciences J.*, *1*(1), 65-79.

Vasilev, K., Sah, V. R., Goreham, R. V., Ndi, C., Short, R. D., & Griesser, H. J. (2010). Antibacterial surfaces by adsorptive binding of polyvinyl-sulphonate-stabilized silver nanoparticles. *Nanotechnology*, *21*(21), 215102.

Washington, J. A., & Wood, G. L. (1995). Antimicroibial susceptibility tests: Dilution and disc diffusion methods. *Manual of clinical microbiology*, 1327-1331.

Wayne, P. A. (2013). Performance standards for antimicrobial susceptibility testing; 23rd informational supplement. *Clinical and Laboratory Standards Institute. CLSI M10U0-S21*.

Zhu, J., Liu, S., Palchik, O., Koltypin, Y., & Gedanken, A. (2000). Shape-controlled synthesis of silver nanoparticles by pulse sonoelectrochemical methods. *Langmuir*, *16*(16), 6396-6399.

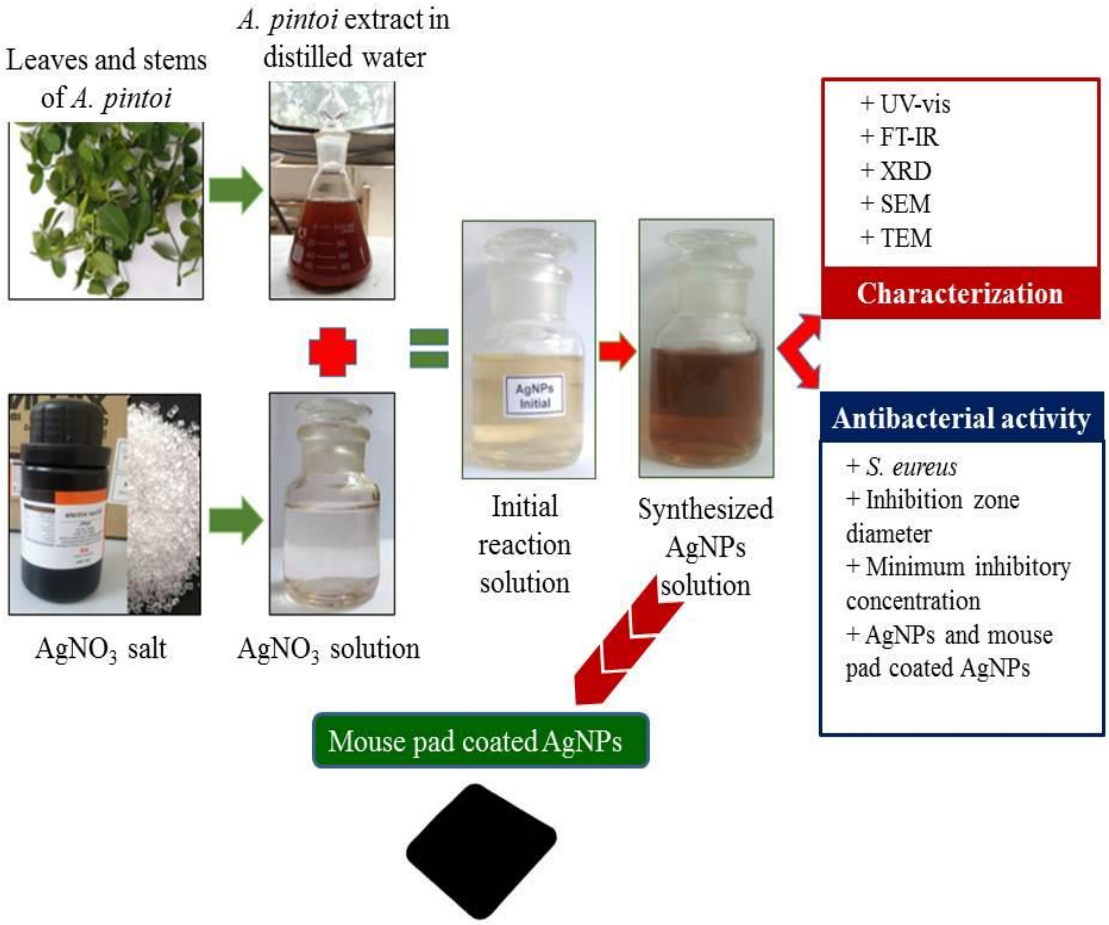

Figure 1. Biosynthesis and characterization of AgNPs using *A. pintoi* extract

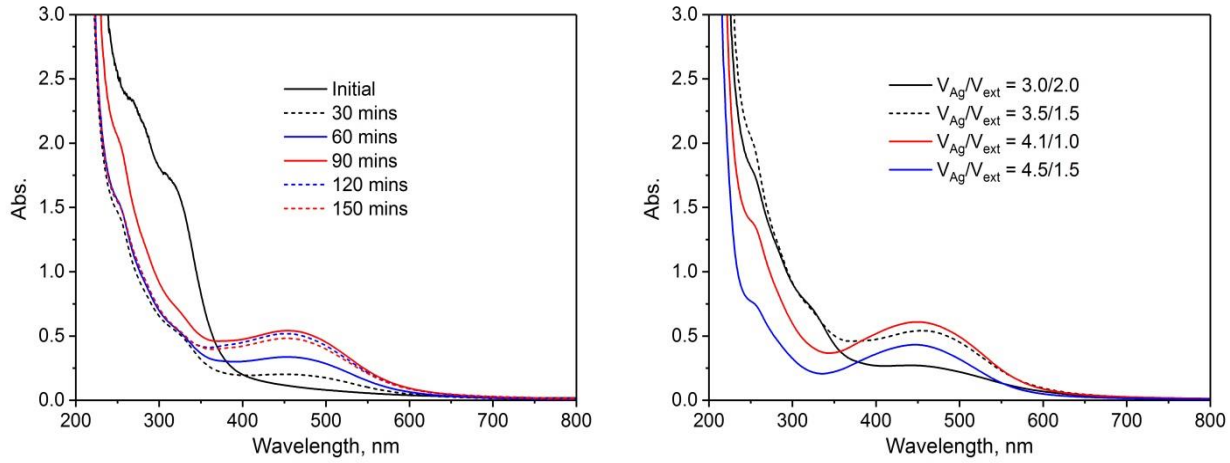

a) b)

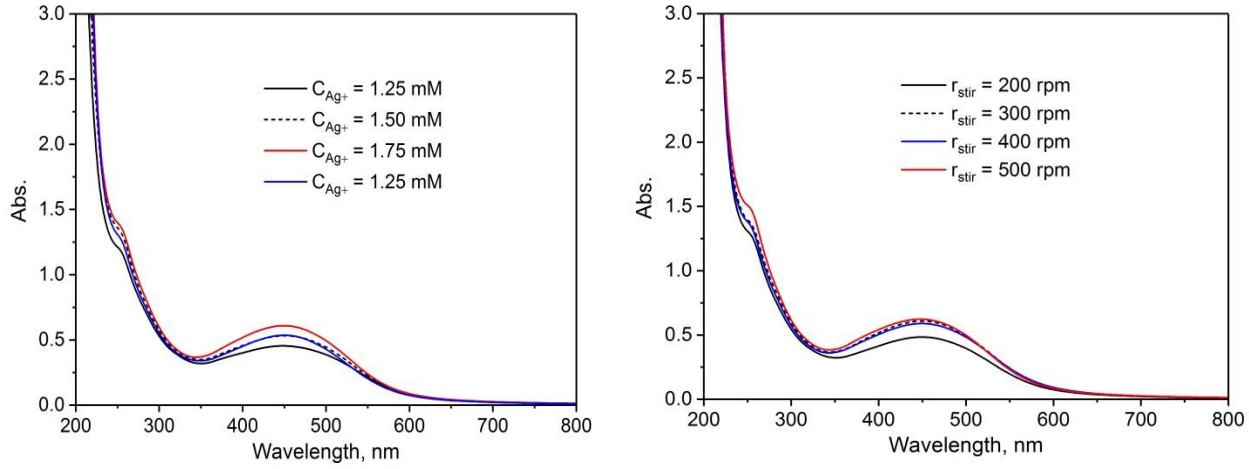

c) d)

Figure 2. UV-Vis spectra of AgNPs suspension samples synthesized at different conditions. a) effect of synthesis duration; b) effect of the volume ratio between $AgNO_3$ solution and extract (V_{Ag}/V_{Ext}); c) effect of $AgNO_3$ concentration; and d) Effect of stirring rate.

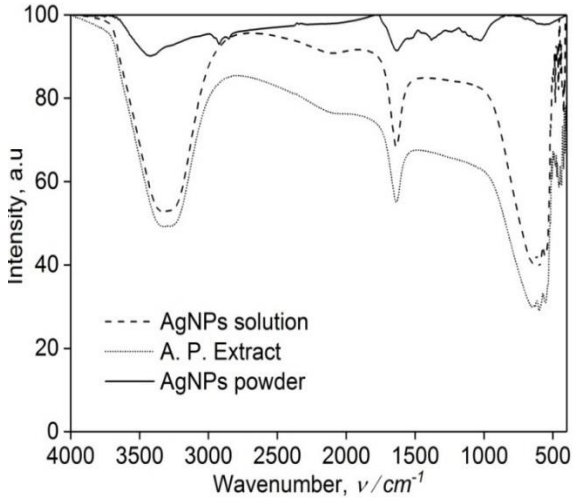

Figure 3. FT-IR spectra of *A. pintoi* extract and AgNPs samples

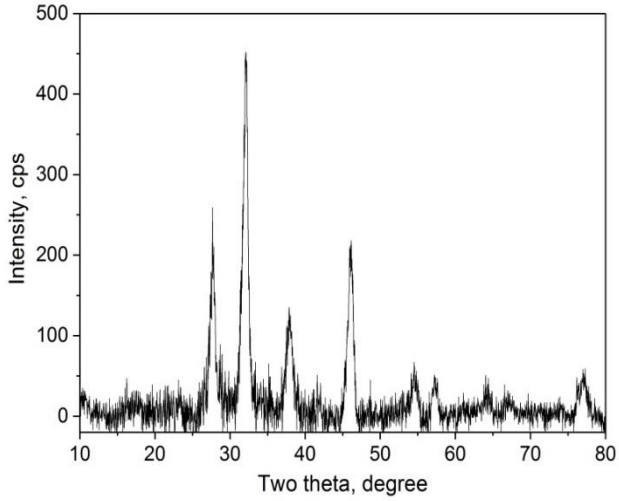

Figure 4. XRD diffraction patterns of synthesized powder AgNPs

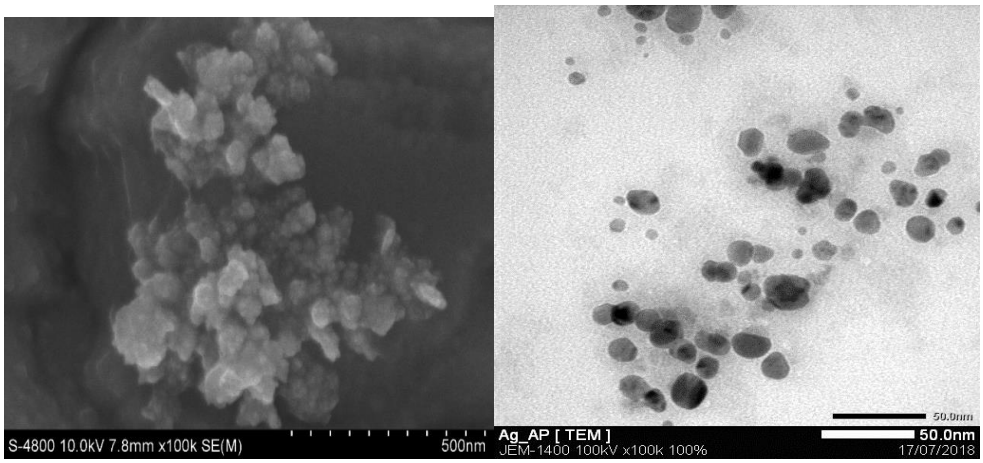

a) b)

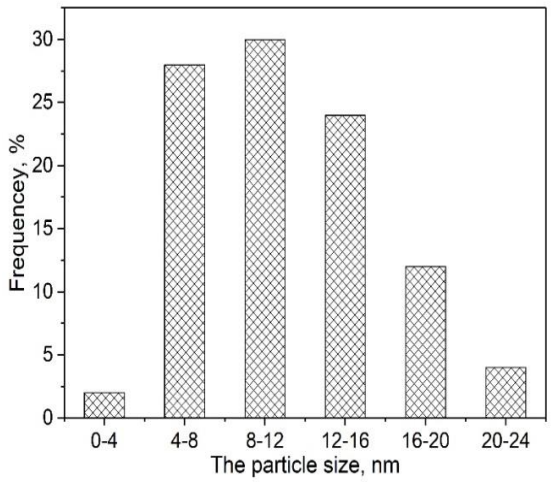

c)

Figure 5. SEM (a), TEM (b) images and the size distribution histogram (c) of AgNPs sample synthesized at the suitable conditions

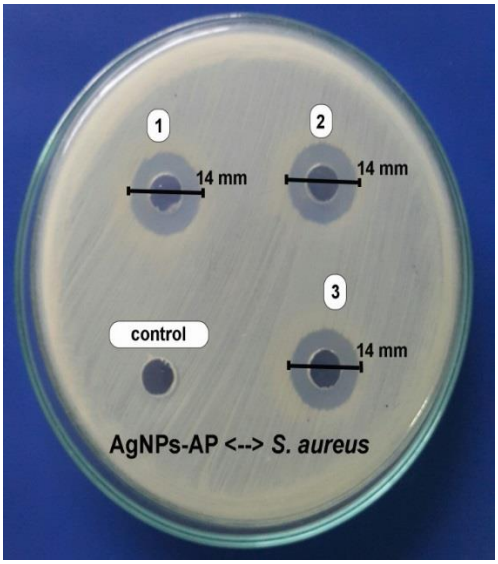

Figure 6. Image of inhibition zone against *S. aureus* of synthesized AgNPs solution

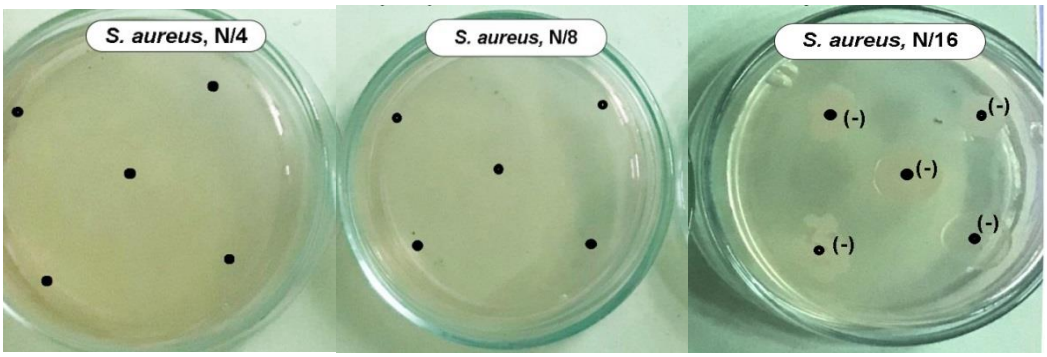

Figure 7. The minimum inhibitory concentration against S. aureus of AgNPs

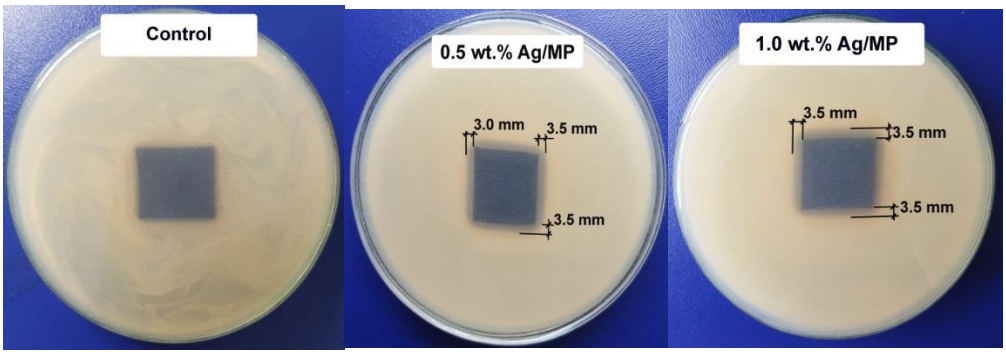

Figure 8. Antibacterial activity of mouse pads coated AgNPs against *S. aureus*.